J. Phys. B: At. Mol. Opt. Phys. **33** (2000) L721–L728. Printed in the UK PII: S0953-4075(00)51004-9

LETTER TO THE EDITOR

Quantal Stark mixing at ultralow collision energies

D Vrinceanu and M R Flannery

School of Physics, Georgia Institute of Technology, Atlanta, GA 30332, USA

Received 9 June 2000, in final form 11 September 2000

Abstract. A new exact solution of the time-dependent quantal equation is obtained for the full array of angular momentum mixing transitions $n\ell \to n\ell'$ in atomic hydrogen induced by collisions with charged particles at ultralow energies. Based on this new solution, efficient numerical procedures are devised. It is proven that the present (fixed-frame) solution is equivalent to the rotating-frame approach described by Kazansky and Ostrovsky (Kazansky A K and Ostrovsky V N 1996 *Phys. Rev. Lett.* **77** 3094) and that it overcomes the difficulties therein. Analytic expressions for low quantum numbers n are presented. Numerical results for the transition array with $n = 28$ are reported.

Stark mixing occurs when the electron of a Rydberg atom (in a state with principal quantum number n) changes its angular momentum ℓ, without changing its energy, as a result of a collision, at large impact parameter b, with a slow massive particle of charge Z_1e moving with velocity v. It is important in many areas of atomic physics, as in the Auger (or autoionization) process which follows the collision between ions and atoms (Miraglia and Macek 1990), in ZEKE spectroscopy (Merkt and Zare 1994), in astrophysics (e.g. Percival 1983), in recent efforts (Mensh'ikov and Fedichev 1995) to produce anti-hydrogen at 4 K and for general three-body recombination (Flannery and Vrinceanu 1998) at ultralow energies. The first stage in ultralow energy electron–ion recombination (Flannery and Vrinceanu 1998) at temperature T_e is a very rapid collisional capture into high Rydberg states with high angular momentum ℓ and large radiative lifetimes at a rate proportional to $T_e^{-4.5}$. Thus the ℓ-mixing is an essential step in producing the low-angular-momentum states required to radiatively decay at a relatively high rate to low levels, thereby stabilizing the recombination.

On considering the Rydberg atom in a frame rotating with the internuclear axis, the Stark mixing problem can be reduced to the problem of the Rydberg atom in mixed *static fields*: electric, provided by the projectile ion, and magnetic, produced by the non-inertial (Coriolis) forces. In this way, the well known equations, in both classical (Born 1960) and quantum (Demkov *et al* 1970) mechanics, for the problem of interaction between weak fields and an atom, can be adopted to provide, in principle, a solution for the Stark mixing problem. Both quantal (Kazansky and Ostrovsky 1996a, b) and classical (Kazansky and Ostrovsky 1996b, c) versions of this approach have succeeded only for $\ell = 0$ to higher angular momentum ℓ' transitions, appropriate to the experiments described in a paper by Sun and MacAdam (1993).

This letter presents a new exact solution for the Stark mixing process, valid for transitions $n\ell \to n\ell'$ between *any states* within the shell of energy E_n. The present theory in the fixed-frame representation is shown to be formally equivalent to the rotating-frame approach (Kazansky and Ostrovski 1996a, b), but, in contrast to it, the full array of transition amplitudes can be obtained at once by efficient numerical procedures. Results for transitions within the

$n = 28$ energy shell are presented. Analytical formulae for the transition probabilities are possible for low n.

The trajectory of the projectile, initially moving along the positive Z direction, is assumed to be confined in the YOZ plane. In addition to the Hamiltonian $H_0 = p^2/2m_e - e^2/r$, the angular momentum $\boldsymbol{L} = \boldsymbol{r} \times \boldsymbol{p}$ of the unperturbed Rydberg electron and the Runge–Lenz (or eccentricity) vector,

$$\boldsymbol{A} = \left[p^2\boldsymbol{r} - (\boldsymbol{p}\cdot\boldsymbol{r})\boldsymbol{p} - m_e e^2\frac{\boldsymbol{r}}{r}\right]\Big/\, p_n, \tag{1}$$

directed toward the pericentre and normalized to angular momentum units, are also conserved. Here $p_n = \sqrt{-2m_e E_n}$. These quantities define the dynamic $SO(4)$ symmetry of the hydrogen atom. Because the $SO(4)$ group is isomorphic with the direct product $SO(3) \oplus SO(3)$ of two rotation groups, a special decomposition, $\boldsymbol{L} = \boldsymbol{M}+\boldsymbol{N}$ and $\boldsymbol{A} = \boldsymbol{M}-\boldsymbol{N}$, permits the dynamics of the hydrogen atom to be separated into two decoupled motions. The generators $\boldsymbol{M}$ and $\boldsymbol{N}$ act independently as angular momenta and are also conserved quantities for the unperturbed Rydberg atom.

The orbital electron interacts with the time-dependent electric field $\vec{\mathcal{E}}(t)$ generated by the passing projectile of charge Z_1e^2. In the weak-field approximation, this field is constant over the spatial extension of the atom. In this approximation, which is the same as the dipole approximation, the interaction potential $V = e\vec{r}\cdot\vec{\mathcal{E}}$ is

$$V(\boldsymbol{r}, \boldsymbol{R}) = -Z_1e^2\frac{\boldsymbol{R}\cdot\boldsymbol{r}}{R^3} = \frac{Z_1e^2}{vb}\frac{\mathrm{d}\Phi}{\mathrm{d}t}\hat{R}\cdot\boldsymbol{r} = \frac{Z_1e^2}{vb}\frac{\mathrm{d}\Phi}{\mathrm{d}t}(y\sin\Phi + z\cos\Phi) \tag{2}$$

where $\boldsymbol{R}$ is the internuclear vector and Φ is the angle between $\boldsymbol{R}$ and the OZ-axis. The angular momentum of relative motion $L_{\mathrm{rel}} = \mu R^2\dot{\Phi} = \mu vb$, where μ is the reduced mass of the projectile–target system, remains conserved since $L_{\mathrm{rel}} \gg L$, so L_{rel} and L are effectively decoupled. A classical trajectory for the relative motion is then valid.

If the projectile moves very slowly, the orbital electron adjusts itself adiabatically to the ion perturbation and no energetic transitions occur. In this limit, Pauli's replacement rule $\boldsymbol{r} \approx \langle\boldsymbol{r}\rangle = -3\boldsymbol{A}/2p_n$ is valid within the n energy shell (see Vrinceanu and Flannery (2000) for a detailed explanation). The perturbing potential (2) can then be written in terms of the components A_2 and A_3 as

$$V(\alpha) = -\alpha\frac{\mathrm{d}\Phi}{\mathrm{d}t}(A_2\sin\Phi + A_3\cos\Phi)$$

where the Stark parameter $\alpha = 3Z_1a_nv_n/2bv$ and a_n and v_n are the average electron-orbit radius and velocity.

The Schrödinger equation for the time evolution operator $U(t, t_0)$ is

$$\mathrm{i}\hbar\frac{\partial U}{\partial t} = (H_0 + V)U \tag{3}$$

where H_0 is the free atom Hamiltonian and V is the interaction potential (2). The position operator and hence the perturbation potential (2) commute with the unperturbed Hamiltonian, as one can prove directly from the matrix elements of the commutator $[\boldsymbol{r}, H_0]$ between any states within the energy E_n shell. The potential in the interaction representation

$$V_{\mathrm{I}} = \mathrm{e}^{\mathrm{i}H_0t/\hbar}V\mathrm{e}^{-\mathrm{i}H_0t/\hbar}$$

is then identical with the potential in the Schrödinger representation ($V_{\mathrm{I}} = V$). The equation to be solved, in the interaction representation, is

$$\mathrm{i}\hbar\frac{\partial U_{\mathrm{I}}}{\partial t} = -\alpha\frac{\mathrm{d}\Phi}{\mathrm{d}t}(A_2\sin\Phi + A_3\cos\Phi)U_{\mathrm{I}} \tag{4}$$

where $U_{\mathrm{I}}(t, t_0) = \exp(\mathrm{i}H_0 t/\hbar) U \exp(-\mathrm{i}H_0 t_0/\hbar)$. Because the set of operators $\{L_1, A_2, A_3\}$ is closed under the commutation operation and generates the rotation group $SO(3)$, the solution of equation (4) is obtained in terms of elements of this group as

$$U_{\mathrm{I}}(t, t_0) = \mathrm{e}^{\mathrm{i}\Phi L_1/\hbar} \exp[-\mathrm{i}(\Phi - \Phi_0)(L_1 - \alpha A_3)/\hbar] \mathrm{e}^{-\mathrm{i}\Phi_0 L_1/\hbar}. \tag{5}$$

Impact angles Φ and Φ_0 correspond to the position of the projectile at times t and t_0, respectively. The above solution (5) can be easily verified with the aid of the relations

$$\begin{aligned}
\mathrm{e}^{\mathrm{i}\lambda A_2/\hbar} L_1 \mathrm{e}^{-\mathrm{i}\lambda A_2/\hbar} &= L_1 \cos\lambda + A_3 \sin\lambda \\
\mathrm{e}^{\mathrm{i}\lambda A_2/\hbar} A_3 \mathrm{e}^{-\mathrm{i}\lambda A_2/\hbar} &= A_3 \cos\lambda - L_1 \sin\lambda \\
\mathrm{e}^{\mathrm{i}\lambda L_1/\hbar} A_3 \mathrm{e}^{-\mathrm{i}\lambda L_1/\hbar} &= A_3 \cos\lambda + A_2 \sin\lambda
\end{aligned}$$

which are derived from the basic identity

$$\mathrm{e}^{\lambda A} B \mathrm{e}^{-\lambda A} = B + \frac{\lambda}{1!}[A, B] + \frac{\lambda^2}{2!}[A, [A, B]] + \cdots \tag{6}$$

and the commutation relations $[L_1, A_2] = \mathrm{i}\hbar A_3$, $[L_1, A_3] = -\mathrm{i}\hbar A_2$ and $[A_2, A_3] = \mathrm{i}\hbar L_1$. The initial condition $U(t_0, t_0) = \mathbf{1}$ is automatically satisfied. Note, in the limit as $\alpha \to 0$, that $U(t_0, t) = \mathbf{1}$ for all time and no (l, m) transitions can then occur.

The transition amplitude for a Stark mixing process is

$$a_{\beta\alpha}^{(n)} = \langle n\beta | U_{\mathrm{I}}(\infty, -\infty) | n\alpha \rangle \tag{7}$$

where the initial unperturbed state $|n\alpha\rangle$, at $t = -\infty$, evolves to the final states $|n\beta\rangle$, at $t = \infty$. Since α and β label the states within the same energy shell, the superscript n can be omitted and all dynamics is restricted to the energy shell defined by quantum number n. The full array of transition amplitudes is given by equation (5) in (7) and is feasible and efficient for practical numerical applications since it requires only matrix operations.

The core of solution (5) is the exponential of the operator $L_1 - \alpha A_3$. By using basic commutator algebra, Pauli's replacement and equation (6), this operator can be diagonalized as

$$\mathrm{e}^{-\mathrm{i}yq/\hbar}(L_1 - \alpha A_3)\mathrm{e}^{\mathrm{i}yq/\hbar} = \gamma L_1$$

where $q = (2p_n/3) \arctan\alpha$ and $\gamma = \sqrt{1 + \alpha^2}$. The solution (5) has therefore the alternative form

$$U_{\mathrm{I}}(t, t_0) = \mathrm{e}^{\mathrm{i}\Phi L_1/\hbar} \mathrm{e}^{-\mathrm{i}yq/\hbar} \mathrm{e}^{-\mathrm{i}\gamma(\Phi - \Phi_0)L_1/\hbar} \mathrm{e}^{\mathrm{i}yq/\hbar} \mathrm{e}^{-\mathrm{i}\Phi_0 L_1/\hbar} \tag{8}$$

which illustrates quite nicely how the action of the slow distant encounter charged projectile incident along the negative Z-axis can be decomposed into successive rotations about the X-axis and alternating impulsive momentum transfers $\pm q(\alpha)$ along the Y-axis. In the limit of zero impulse q, (8) is unitary and no transitions occur. In the limit of small Stark parameter α the above solution (8), for undeflected collisions $\Delta\Phi \equiv (\Phi - \Phi_0) = -\pi$, reduces to

$$U_{\mathrm{I}} = \mathrm{e}^{-2\mathrm{i}qy/\hbar} + \mathrm{O}(\alpha^2)$$

in agreement with the impulsive result (Vrinceanu and Flannery 2000).

It is however interesting to note that by introducing the Pauli replacement directly in the potential (2) and by writing the Runge–Lenz vector as $\boldsymbol{A} = \boldsymbol{M} - \boldsymbol{N}$, the potential decomposes as

$$V = V_M + V_N$$

where $V_M = -\alpha(M_2 \sin\Phi + M_3 \cos\Phi)\dot{\Phi}$ and $V_N = \alpha(N_2 \sin\Phi + N_3 \cos\Phi)\dot{\Phi}$. Because the commutators $[M_i, N_j]$, $[M_i, H_0]$ and $[N_i, H_0] = 0$ (for any $i, j = 1, 2, 3$ combination), the

Table 1. The four bases useful for describing the quantal states of the hydrogen atom.

Basis	Quantum numbers	Complete set of commuting observables	Origin
Orbital	$\vert n\ell m\rangle_{\mathrm{O}}$	H_0, L^2, L_3	Standard for spherical coordinates; describes correctly the states of the field-free atom
Parabolic	$\vert n_1 n_2 m\rangle_{\mathrm{P}}$	H_1, H_2, L_3	Separation of Hamiltonian $H = H_1 + H_2$ in parabolic coordinates, $\xi = r + z$, $\eta = r - z$, $\tan\varphi = y/x$; $n = n_1 + n_2 + \vert m\vert + 1$
Stark	$\vert nqm\rangle_{\mathrm{S}}$	H_0, A_3, L_3	Parabolic basis; describes the Stark states for small electric field $\mathcal{E}$, when the interaction $-e\mathcal{E}z$ is diagonal; $q = n_1 - n_2$
Algebraic	$\vert n\mu\nu\rangle_{\mathrm{A}}$	H_0, M_3, N_3	The two rotation groups in which the dynamic symmetry group $SO(4) \equiv SO(3) \oplus SO(3)$ decomposes; the equivalent angular momentum for both $SO(3)$ representations is $j = (n-1)/2$; $\mu = (m+q)/2$ and $\nu = (m-q)/2$

problem (3) becomes separable, in exactly the same way as the classical Stark mixing equations can be decoupled (Vrinceanu and Flannery 2000). The time evolution operator then factorizes as

$$U = U_{H_0} U_M U_N \tag{9}$$

where, of course, $U_{H_0} = \exp(-\mathrm{i}H_0(t-t_0)/\hbar)$ and both U_M and U_N are solutions of equations $\mathrm{i}\hbar\partial U_M/\partial t = V_M U_M$ and $\mathrm{i}\hbar\partial U_N/\partial t = V_N U_N$, similar to equation (3). With the aid of the group theoretical result (5), the solutions for the operators U_M and U_N are then

$$U_M = \mathrm{e}^{\mathrm{i}\Phi M_1/\hbar} \exp[-\mathrm{i}/\hbar(\Phi - \Phi_0)(M_1 - \alpha M_3)]\mathrm{e}^{-\mathrm{i}\Phi_0 M_1/\hbar} \tag{10}$$

and

$$U_N = \mathrm{e}^{\mathrm{i}\Phi N_1/\hbar} \exp[-\mathrm{i}/\hbar(\Phi - \Phi_0)(N_1 + \alpha N_3)]\mathrm{e}^{-\mathrm{i}\Phi_0 N_1/\hbar}. \tag{11}$$

In calculating the amplitude (7), four interesting basis sets can be chosen for the one-electron hydrogen-like atom. Table 1 summarizes key properties of these bases. The orbital basis is useful for describing the field-free atom, before and after the collision, whereas the algebraic basis appears naturally as a basis where M_3 and N_3 are diagonal. The solution (9) has the simplest expression in this algebraic basis. All four bases in table 1 span the n^2 degenerate energy shell and can be equally adopted to characterize the hydrogen atom. The algebraic basis spans a tensorial product of two spaces ($|\mu\rangle \otimes |\nu\rangle$) corresponding to spaces used for matrix representation of the product $SO(3) \oplus SO(3)$. The two spaces have the same dimension because $M^2 = N^2 = L^2 + A^2 = (n^2-1)\hbar^2$ and are associated with two angular momenta with $j = (n-1)/2$.

The transition amplitude between the two algebraic states is then the product $a_{(\mu'\nu'),(\mu\nu)} = a_{\mu'\mu}a_{\nu'\nu}$ of two amplitudes for M and N independent actions. Each factor is the matrix element of a $j = (n-1)/2$-dimensional representation of the rotations represented by equations (10) and (11). For example, from (10), one obtains $a_{\mu'\mu} = F(\alpha)_{\mu'\mu}$, with

$$F(\alpha) = \mathcal{D}^{(j)}[-\Phi, (1,0,0)]\mathcal{D}^{(j)}\left[\gamma\Delta\Phi, \left(\frac{1}{\gamma}, 0, -\frac{\alpha}{\gamma}\right)\right]\mathcal{D}^{(j)}[\Phi_0, (1,0,0)]$$

where $\mathcal{D}[\phi, (n_1, n_2, n_3)]$ is the Wigner matrix representation for the rotation $\mathcal{R}(\phi, \boldsymbol{n})$ with angle ϕ about direction $\boldsymbol{n}$ (see Louck (1996) for the explicit expression). $\Delta\Phi$ is the polar angle $\Phi - \Phi_0$ swept out during the interaction. The transition probability in the space of $\boldsymbol{N}$ is the element $\nu'\nu$ of the matrix $F(-\alpha)$.

Calculation of the transition probability between orbital states requires the explicit unitary transformation between the orbital and algebraic bases. This can be obtained by direct scalar products of the orbital and parabolic states for which explicit coordinate representations are known. The result may be written in terms of hypergeometric functions (Tarter 1970). However, an equivalent result is provided by the $SO(4) \approx SO(3) \oplus SO(3)$ isomorphism. The orbital state, as a combination of two angular momentum states, is

$$|n\ell m\rangle = \sum_{\mu,\nu=-j}^{j} C_{\mu\nu}^{(\ell m)} |n\mu\nu\rangle$$

where the transformation matrix $C^{(\ell m)}$ is given by the standard Clebsch–Gordan coefficients $\langle j\mu j\nu|\ell m\rangle$. The transition probability for the $\ell m \to \ell' m'$ transition then becomes

$$a_{\ell' m',\ell m} = \sum_{\mu\nu\mu'\nu'} C_{\mu'\nu'}^{(\ell' m')} C_{\mu\nu}^{(\ell m)} F_{\mu'\mu}(\alpha) F_{\nu'\nu}(-\alpha) \tag{12}$$

which can be expressed in matrix form as

$$a_{\ell' m',\ell m} = \mathrm{Trace}[C^{(\ell' m')} F(-\alpha) C^{(\ell m)^T} F^T(\alpha)]$$

where C^T is the transpose of matrix C. This result (12) is in exact agreement with the solution obtained by Kazansky and Ostrovsky (1996a, b), who used the rotating-frame approach.

The quantal development above is exquisite in that it follows exactly the same reasoning within the exact classical mechanics solution (Vrinceanu and Flannery 2000). This result exhibits the essential power of the $SO(4)$ symmetry group for the energy shell of the hydrogen atom. The common $SO(4)$ symmetry therefore transcends the chosen formulation (classical or quantal) and provides a classical–quantal correspondence at a level more fundamental than Ehrenfest's theorem and the Heisenberg correspondence.

In practice, the fourfold summation (12) and the use of the Wigner rotation matrices $\mathcal{D}$ in $F(\alpha)$ are not very efficient and the difficulty of calculation increases dramatically with n. Instead, the solution (5) provides a much simpler approach, because the matrix elements of the argument in the exponential have simple expressions directly in the orbital basis. The array of transitions is obtained at once, all within one matrix exponentiation of a band diagonal matrix for which efficient algorithms are available (see e.g. Golub and Loan 1983).

When the projection of the initial and final angular momentum is not determined, the transition probability is

$$P_{\ell'\ell}(\alpha) = \frac{1}{2\ell+1} \sum_{m=-\ell}^{\ell} \sum_{m'=-\ell'}^{\ell'} |a_{\ell' m',\ell m}|^2.$$

The present theory is now applied in the following paragraphs for low $n = 2$ and 3, when analytic results can be derived, and for $n = 28$, when accurate numerical results can be obtained. A matrix representation for the operator $L_1 - \alpha A_3$ is required. Instead of the spherical basis $|\ell m\rangle$, which is difficult to use in this case, we define a new linear basis obtained by mapping the (l, m) quantum numbers to a unique index $k = \ell^2 + \ell + m + 1$, in such a way that $(0, 0) \to 1$, $(1, -1) \to 2$, $(1, 0) \to 3$, $(1, 1) \to 4$, $(2, -2) \to 5$ and so on. The inverse mapping is given by $\ell = \mathrm{floor}(\sqrt{k-1})$ and $m = k - \ell^2 - \ell - 1$. The index k counts the degeneracy of the energy shell, and runs from 1 to n^2. The matrix element

$$(L_1)_{\ell m}^{\ell' m'} = \sqrt{(\ell+m)(\ell-m+1)}/2\delta_{\ell'\ell}\delta_{m',m-1} + \sqrt{(\ell-m)(\ell+m+1)}/2\delta_{\ell'\ell}\delta_{m',m+1}$$

of L_1 is non-zero only for $\Delta\ell = 0$ and $\Delta m = \pm 1$, which reflects the fact that the cylindrical symmetry of the Rydberg atom is broken by the precession of $\boldsymbol{L}$ about the field of the projectile. These m-changing transitions are however conditioned by the full structure of solution (5)

$$\begin{array}{ccc}
 & \begin{array}{ccccccccc} l' & 0 & 1 & & & 2 & & & \\ m' & 0 & -1 & 0 & 1 & -2 & -1 & 0 & 1 \; 2 \end{array} & \\
\begin{array}{cc} l & m \\ 0 & 0 \\ & -1 \\ 1 & 0 \\ & 1 \\ & -2 \\ & -1 \\ 2 & 0 \\ & 1 \\ & 2 \end{array} &
\begin{pmatrix}
0 & 0 & 2\alpha\sqrt{2/3} & 0 & 0 & 0 & 0 & 0 & 0 \\
0 & 0 & 1/\sqrt{2} & 0 & 0 & \alpha & 0 & 0 & 0 \\
2\alpha\sqrt{2/3} & 1/\sqrt{2} & 0 & 1/\sqrt{2} & 0 & 0 & 2\alpha/\sqrt{3} & 0 & 0 \\
0 & 0 & 1/\sqrt{2} & 0 & 0 & 0 & 0 & \alpha & 0 \\
0 & 0 & 0 & 0 & 0 & 1 & 0 & 0 & 0 \\
0 & \alpha & 0 & 0 & 1 & 0 & \sqrt{3/2} & 0 & 0 \\
0 & 0 & 2\alpha/\sqrt{3} & 0 & 0 & \sqrt{3/2} & 0 & \sqrt{3/2} & 0 \\
0 & 0 & 0 & \alpha & 0 & 0 & \sqrt{3/2} & 0 & 1 \\
0 & 0 & 0 & 0 & 0 & 0 & 0 & 1 & 0
\end{pmatrix} &
\begin{array}{c} 1 \\ 2 \\ 3 \\ 4 \\ 5 \\ 6 \\ 7 \\ 8 \\ 9 \end{array} \\
 & \begin{array}{ccccccccc} 1 & 2 & 3 & 4 & 5 & 6 & 7 & 8 & 9 \end{array} &
\end{array}$$

Figure 1. Matrix representation of $L_1 - \alpha A_3$ for $n = 3$.

which shows that such transitions are only in evidence for non-zero α. The matrix element

$$(A_3)_{\ell m}^{\ell' m'} = -\sqrt{\frac{(\ell^2 - m^2)(n^2 - \ell^2)}{(2\ell + 1)(2\ell - 1)}}\,\delta_{\ell' \ell - 1}\delta_{m',m} - \sqrt{\frac{[(\ell + 1)^2 - m^2][n^2 - (\ell + 1)^2]}{(2\ell + 3)(2\ell + 1)}}\,\delta_{\ell' \ell + 1}\delta_{m',m}$$

of the component $A_3 = -(2/3n)z$ along the fixed Z-axis of quantization is non-zero for $\Delta\ell = \pm 1$ and $\Delta m = 0$ transitions. These dipole transitions only contribute for non-zero α. The matrix $L_1 - \alpha A_3$ has therefore the band diagonal structure, as illustrated in figure 1 for the special case of $n = 3$. The transition amplitude for transition $k \to k'$ is the kk' matrix element of the exponential of the matrix $-\mathrm{i}\Delta\Phi(L_1 - \alpha A_3)$, sandwiched between the rotations implied by (5). When $\alpha \approx 0$, the dipole-forbidden transitions are not possible because the transition matrix $\approx \exp -\mathrm{i}\Delta\Phi L_1$ still has a band diagonal structure. When α increases, more and more off-diagonal elements become populated, resulting in an increasing number of dipole-forbidden transitions with $\Delta\ell = \ell' - \ell$ and $\Delta m = m' - m$. Efficient algorithms, using Padé approximations, are available (Golub and Loan 1983) for matrix exponentiation. The whole array of transition probabilities for all ℓ and $\ell'$is then obtained at once.

Analytical probabilities for $\ell \to \ell'$ transitions within the $n = 2$ shell are listed below:

$$P_{00}^{(2)} = \left(\frac{1}{\gamma^4}\right)[1 + \alpha^2 \cos(\gamma\Delta\Phi)]^2$$

$$P_{01}^{(2)} = \left(\frac{2\alpha^2}{3\gamma^4}\right)[2 + \alpha^2 + \alpha^2 \cos(\gamma\Delta\Phi)] \sin^2\left(\frac{\gamma\Delta\Phi}{2}\right)$$

$$P_{11}^{(2)} = \left(\frac{1}{6\gamma^4}\right)[6 + 8\alpha^2 + 5\alpha^4 + 4\alpha^2 \cos(\gamma\Delta\Phi) + \alpha^4 \cos(2\gamma\Delta\Phi)].$$

The following transition probabilities for the $n = 3$ shell are also obtained:

$$P_{00}^{(3)} = \left(\frac{1}{9\gamma^8}\right)[3 - 2\alpha^2 + \alpha^4 + 8\alpha^2 \cos(\gamma\Delta\Phi) + 2\alpha^4 \cos(2\gamma\Delta\Phi)]^2$$

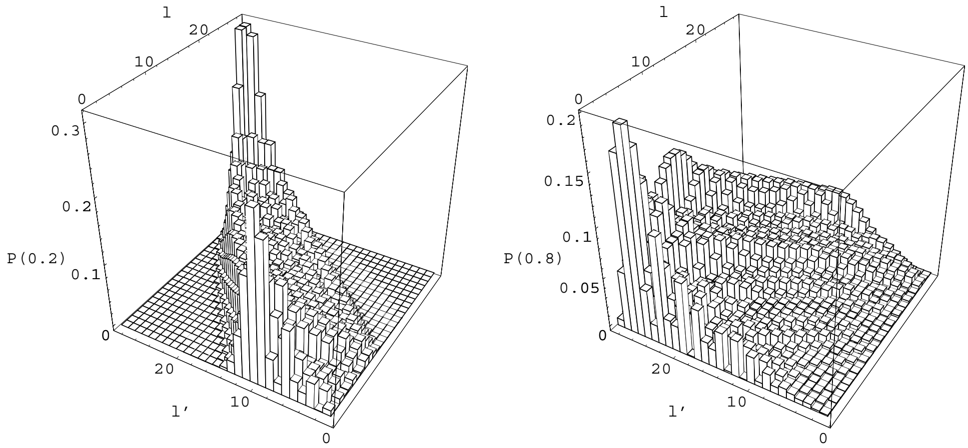

Figure 2. Stark mixing transition probabilities for the $28\ell \rightarrow 28\ell'$ transition array, with $\alpha = 0.2$ (left) and $\alpha = 0.8$ (right).

$$
\begin{aligned}
P_{01}^{(3)} &= \left(\frac{16\alpha^2}{9\gamma^8}\right)[1+\alpha^2\cos(\gamma\Delta\Phi)]^2[2+\alpha^2+\alpha^2\cos(\gamma\Delta\Phi)]\sin^2\left(\frac{\gamma\Delta\Phi}{2}\right)\\
P_{02}^{(3)} &= \left(\frac{32\alpha^4}{45\gamma^8}\right)[2+\alpha^2+\alpha^2\cos(\gamma\Delta\Phi)]^2\sin^4\left(\frac{\gamma\Delta\Phi}{2}\right)\\
P_{11}^{(3)} &= \left(\frac{1}{6\gamma^8}\right)[(6+30\alpha^4+4\alpha^6+3\alpha^8)+8\alpha^2(3-2\alpha^2+2\alpha^4)\cos(\gamma\Delta\Phi)\\
&\quad +2\alpha^4(11-2\alpha^2+\alpha^4)\cos(2\gamma\Delta\Phi)+8\alpha^6\cos(3\gamma\Delta\Phi)+\alpha^8\cos(4\gamma\Delta\Phi)]\\
P_{12}^{(3)} &= \left(\frac{2\alpha^2}{15\gamma^8}\right)[(20+34\alpha^2+32\alpha^4+8\alpha^6)+\alpha^2(26+20\alpha^2+9\alpha^4)\cos(\gamma\Delta\Phi)\\
&\quad +2\alpha^4(4+\alpha^2)\cos(2\gamma\Delta\Phi)+\alpha^6\cos(3\gamma\Delta\Phi)]\sin^2\left(\frac{\gamma\Delta\Phi}{2}\right)\\
P_{22}^{(3)} &= \left(\frac{1}{90\gamma^8}\right)[(90+240\alpha^2+318\alpha^4+196\alpha^6+63\alpha^8)\\
&\quad +8\alpha^2(15+22\alpha^2+14\alpha^4)\cos(\gamma\Delta\Phi)+2\alpha^4(23+22\alpha^2+13\alpha^4)\cos(2\gamma\Delta\Phi)\\
&\quad +8\alpha^6\cos(3\gamma\Delta\Phi)+\alpha^8\cos(4\gamma\Delta\Phi)].
\end{aligned}
$$

The detailed balance relation

$$(2\ell+1)P_{\ell'\ell}^{(n)} = (2\ell'+1)P_{\ell\ell'}^{(n)}$$

is satisfied by the present treatment, so the $P_{\ell'\ell}^{(n)}$ probabilities for transitions with $\ell' > \ell$ can be obtained.

Figure 2 displays the results for calculation of the transition probabilities inside the $n = 28$ energy shell. An undeflected path ($\Delta\Phi = -\pi$) is assumed. For small $\alpha = 0.2$ only elastic or transitions with small angular momentum transfer $\Delta\ell$ have significant probabilities; a band along the diagonal is exhibited. As ℓ increases, $\Delta\ell$ increases and then decreases as $\ell \rightarrow n-1$. As α increases, the band broadens and larger angular momentum transfers become possible for all ℓ.

The present treatment is valid (a) for weak fields, in evidence for impact parameters $b > b^* = (3Z_1/2)^{1/2}a_n$, which implies Stark parameters $\alpha < \alpha^* = (3Z_1/2)^{1/2}(v_n/v)$, and

(b) for adiabatic collisions when the collision frequency $\dot{\Phi}$ is less than the orbital frequency $\omega_n = v_n/a_n$ of the Rydberg electron, so the Pauli replacement holds. These two conditions combine to yield the partitioning $v < v^* = (3Z_1/2)^{1/2}v_n$ and $b > b^*$ in (v, b)-space for Stark mixing collisions (Flannery and Vrinceanu 1998) for a slow encounter in a dipole field. The limit $v < v^*$ defines our meaning of *ultralow* collision energies. The cross section for Stark mixing is

$$\sigma_{n\ell\to n\ell'} = 2\pi \int_0^\infty P_{\ell'\ell}^{(n)} b\,\mathrm{d}b = 2\pi \left(\frac{3Z_1 a_n}{2v/v_n}\right)^2 \int_0^\infty P_{\ell'\ell}^{(n)}(\alpha, \Delta\Phi)\frac{\mathrm{d}\alpha}{\alpha^3}. \qquad (13)$$

When $v < v^*$ and $b < b^*$, the Stark parameter $\alpha > 1$. Since the transition probabilities are bounded for large α, the contribution to the α-integration is vanishingly small for large α, decreasing as α^{-3}, and can, in practice, be neglected for $\alpha > 1$. This implies that the *lower* limit to b is $b_s = \frac{3}{2}Z_1(v_n/v)a_n$. At ultralow energies, this limit is always much greater than the weak-field limit b^*. At the upper limit $v = v^*$ of ultralow energies, b_s approaches from above the weak-field limit b^*. In practical calculations of (13), various physical effects such as Debye screening in a plasma, quantum defects and spin–orbit coupling determine an *upper* limit to b and hence a lower limit $\alpha_{\min}$ to α. For trajectories with zero deflection ($\Delta\Phi = -\pi$), (13) varies universally as $(Z_1 a_n v_n/v)^2$. Departure from this variation is governed by $\Delta\Phi(b, v)$ and by the physical limits imposed upon the α-integration.

In summary, this letter has presented a new form (5) of the exact quantal solution for the Stark mixing probabilities. Based on this new solution for the whole array of transitions, analytical expressions for small quantum numbers n and accurate numerical results even for large n can be obtained. Using the rich symmetry group of the hydrogen atom, the relation with previously published results (Kazansky and Ostrovsky 1996a, b) has been developed in an exquisite fashion. The symmetry group also provides a complete exact classical solution (Vrinceanu and Flannery 2000), capable of explaining the main features of the quantal results and of providing a quantal–classical (dynamical) correspondence at a level, more fundamental than Ehrenfest's theorem and the Heisenberg correspondence.

This research is supported by grants from AFOSR: F 49620-99-1-0277 and NSF: 98-02622.

References

Born M 1960 *The Mechanics of the Atom* (New York: Ungar) p 235

Demkov Yu N, Monozon B S and Ostrovskiĭ V N 1970 *Sov. Phys.–JETP* **30** 775

Flannery M R and Vrinceanu D 1998 *Atomic Processes in Plasmas: 11th APS Topical Conf.* ed E Oks and M S Pindzola (New York: AIP) pp 317–33

Golub G H and Loan C F V 1983 *Matrix Computation* (Baltimore, MD: John Hopkins University Press) p 384

Kazansky A K and Ostrovsky V N 1996a *Phys. Rev. Lett.* **77** 3094

——1996b *Sov. Phys.–JETP* **83** 1095

——1996c *J. Phys. B: At. Mol. Opt. Phys.* **29** 3651

Louck J D 1996 *Atomic, Molecular, and Optical Physics Handbook* ed G W F Drake (New York: AIP) p 15

Men'shikov L I and Fedichev P O 1995 *Sov. Phys.–JETP* **81** 78

Merkt F and Zare R N 1994 *J. Chem. Phys.* **101** 3495

Miraglia J E and Macek J 1990 *Phys. Rev.* A **42** 3971

Percival I 1983 *Atoms in Astrophysics* ed P G Burke, W B Eissner, D G Hummer and I C Percival (New York: Plenum) p 96

Sun X and MacAdam K B 1993 *Phys. Rev.* A **47** 3913

Tarter C B 1970 *J. Math. Phys.* **11** 3192

Vrinceanu D and Flannery M R 2000 *Phys. Rev.* A submitted